Supporting Information

Synthesis of red/black phosphorus-based composite nanosheets with Z-scheme heterostructure for high-performance cancer phototherapy

*Yong Kang, Zhengjun Li, Fengying Lu, Zhiguo Su, Xiaoyuan Ji, Songping Zhang**

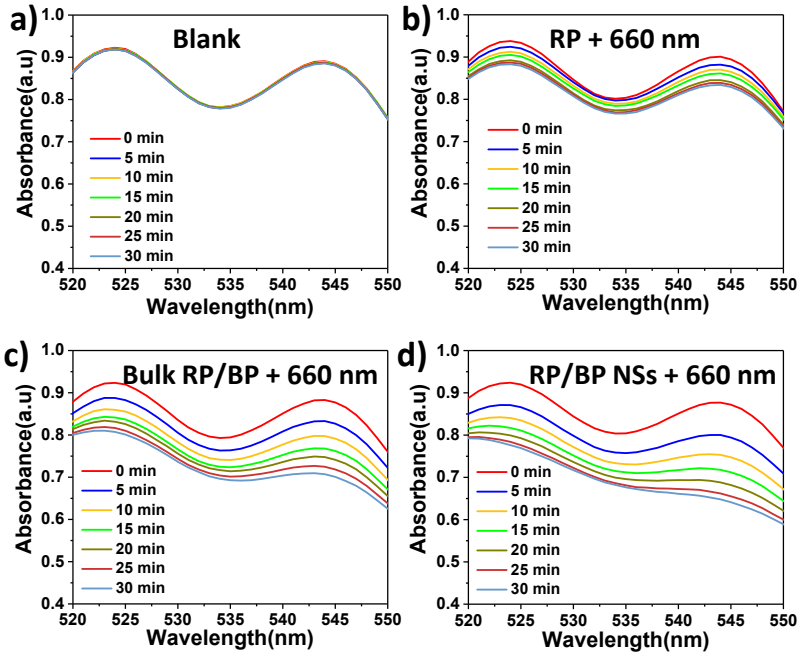

Fig. S1: a) Time dependence of the UV-Vis absorption spectra of $KMnO_4$ solution (0.375 mM) under 660 nm laser irradiation during photocatalytic water splitting. b) Time dependence of the UV-Vis absorption spectra of $KMnO_4$ solution (0.375 mM) in the presence of RP. c) Time dependence of the UV-Vis absorption spectra of $KMnO_4$ solution (0.375 mM) in the presence of bulk RP/BP. d) Time dependence of the UV-Vis absorption spectra of $KMnO_4$ solution (0.375 mM) in the presence of RP/BP NSs.

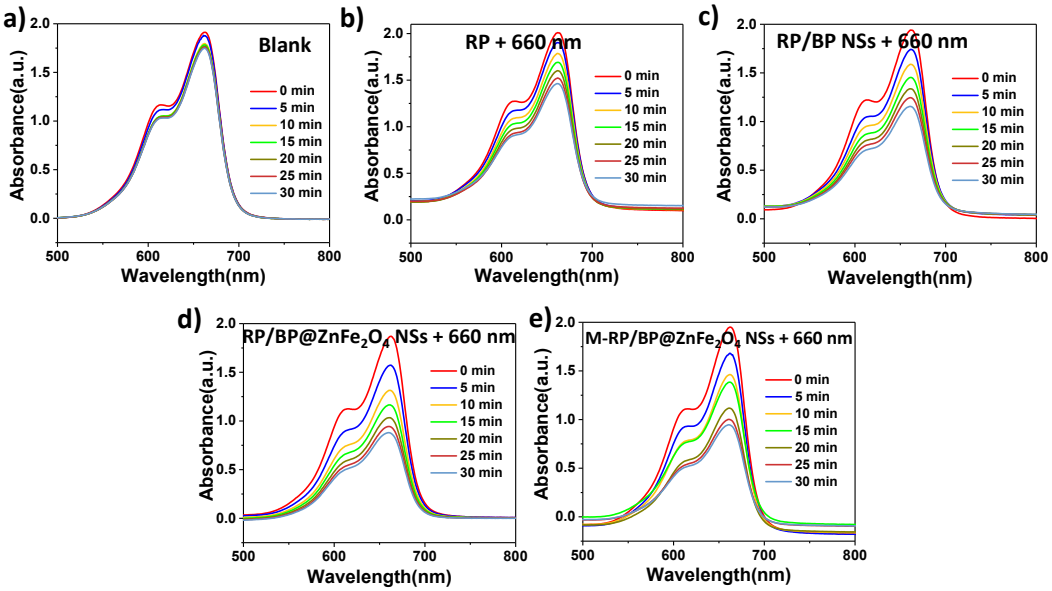

Fig. S2: a) Absorption spectra of MB under 660 nm laser irradiation over different periods of time. b) Absorption spectra of MB treated with RP under 660 nm laser irradiation over different periods of time. c) Absorption spectra of MB treated with RP/BP NSs under 660 nm laser irradiation over different periods of time. d) Absorption spectra of MB treated with RP/BP@$ZnFe_2O_4$ NSs under 660 nm laser irradiation over different periods of time. e) Absorption spectra of MB treated with M-RP/BP@$ZnFe_2O_4$ NSs under 660 nm laser irradiation over different periods of time.

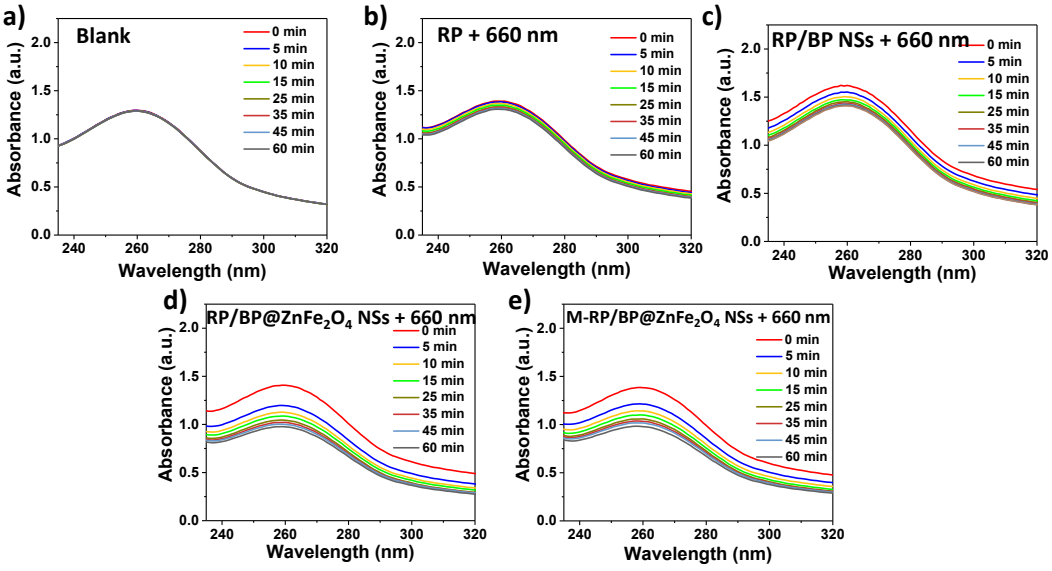

Fig. S3: a) Absorption spectra of NBT under 660 nm laser irradiation over different periods of time. b) Absorption spectra of NBT treated with RP under 660 nm laser irradiation over different periods of time.c) Absorption spectra of NBT treated with RP/BP NSs under 660 nm laser irradiation over different periods of time. d) Absorption

spectra of NBT treated with RP/BP@$ZnFe_2O_4$ NSs under 660 nm laser irradiation over different periods of time. e) Absorption spectra of NBT treated with M-RP/BP@$ZnFe_2O_4$ NSs under 660 nm laser irradiation over different periods of time.

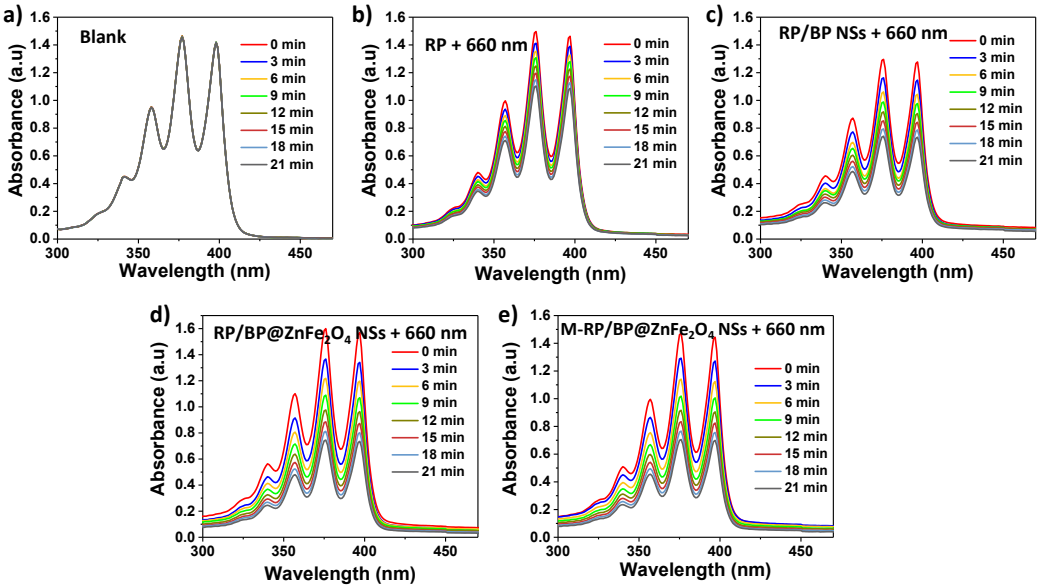

Fig. S4: a) Absorption spectra of ABDA under 660 nm laser irradiation over different periods of time. b) Absorption spectra of ABDA treated with RP under 660 nm laser irradiation over different periods of time. c) Absorption spectra of ABDA treated with RP/BP NSs under 660 nm laser irradiation over different periods of time. d) Absorption spectra of ABDA treated with RP/BP@$ZnFe_2O_4$ NSs under 660 nm laser irradiation over different periods of time. e) Absorption spectra of ABDA treated with M-RP/BP@$ZnFe_2O_4$ NSs under 660 nm laser irradiation over different periods of time.

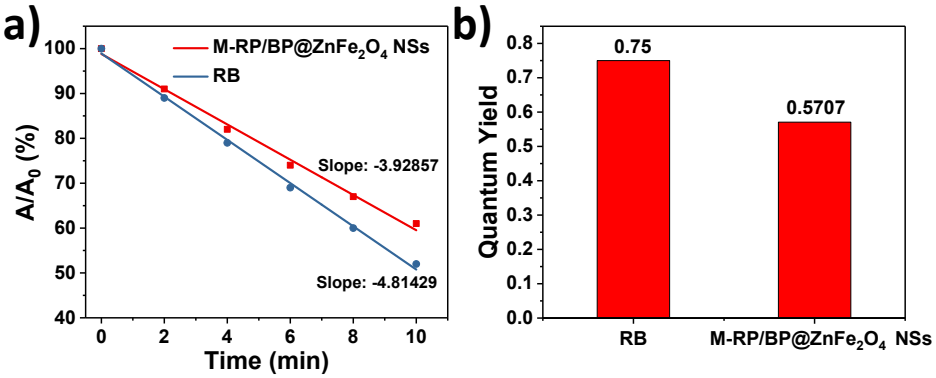

Fig. S5: a) The Lineary fitting of ABDA at 400 nm in the presence of M-RP/BP@$ZnFe_2O_4$ NSs and RB under 808 nm laseer irradiation. b) ROS quantum yields of M-RP/BP@$ZnFe_2O_4$ NSs and RB.

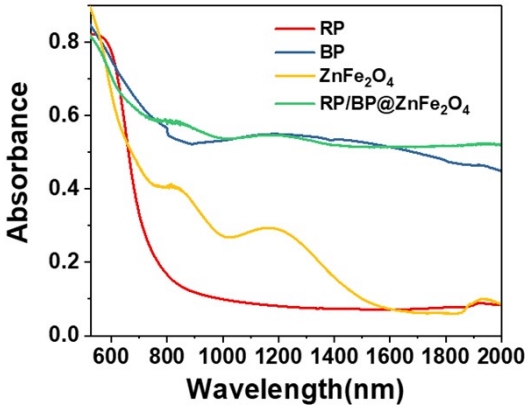

Fig. S6: The UV-vis diffuse-reflectance spectra of the RP, BP, $ZnFe_2O_4$ and RP/BP@ $ZnFe_2O_4$ NSs.

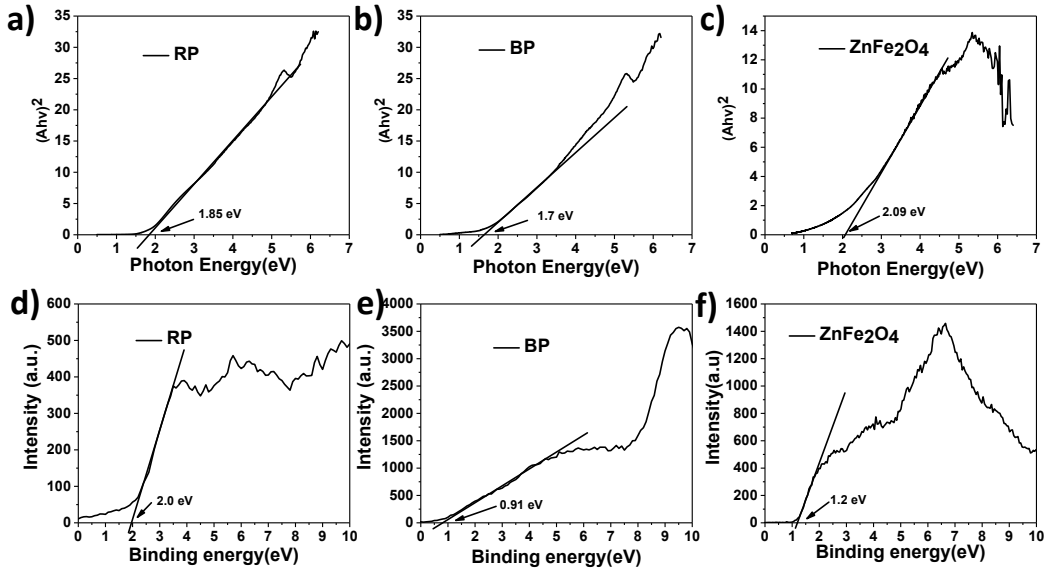

Fig. S7: The corresponding bandgap of a) RP, b) BP, c) $ZnFe_2O_4$ estimated from Kubelka–Munk equation. Valence band XPS spectra of d) RP, e) BP, f) $ZnFe_2O_4$.

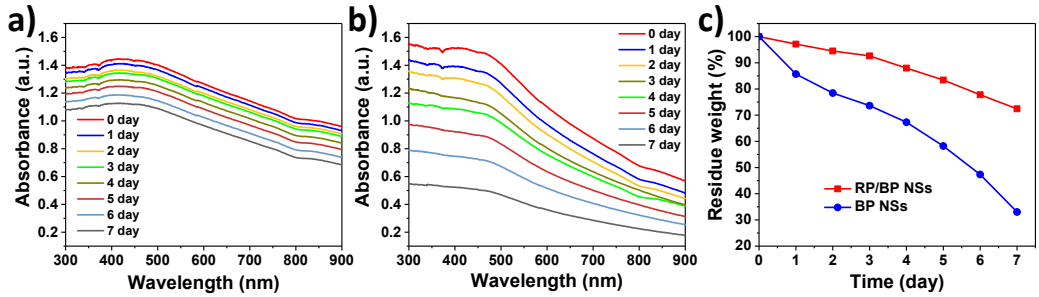

Fig. S8: a) UV-vis-NIR absorption spectra of RP/BP NSs aqueous solution. b) UV-vis-NIR absorption spectra of BP NSs aqueous solution. c) Normalized weight loss of RP/BP NSs and BP NSs at different periods of time.

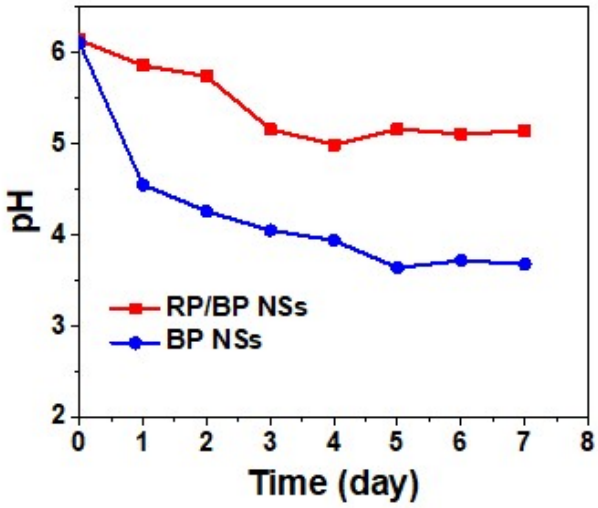

Fig. S9: The pH value detection of BP NSs solution and RP/BP NSs solution for 7 days.

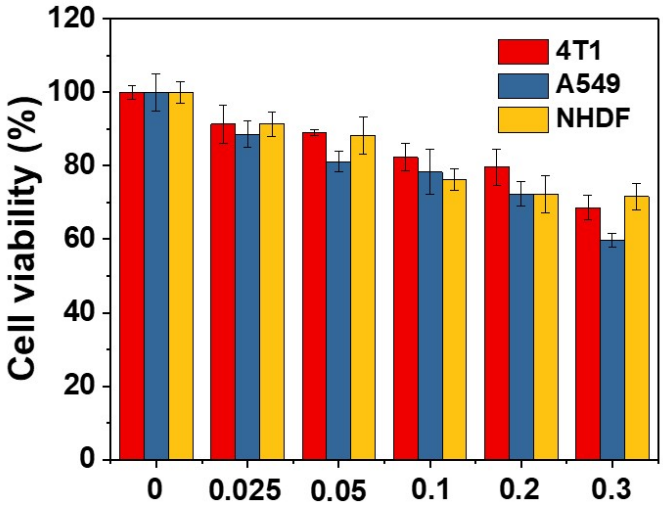

Fig. S10: The cytotoxicity of RP/BP@$ZnFe_2O_4$ NSs in 4T1, A549 and NHDF cells without laser irradiation

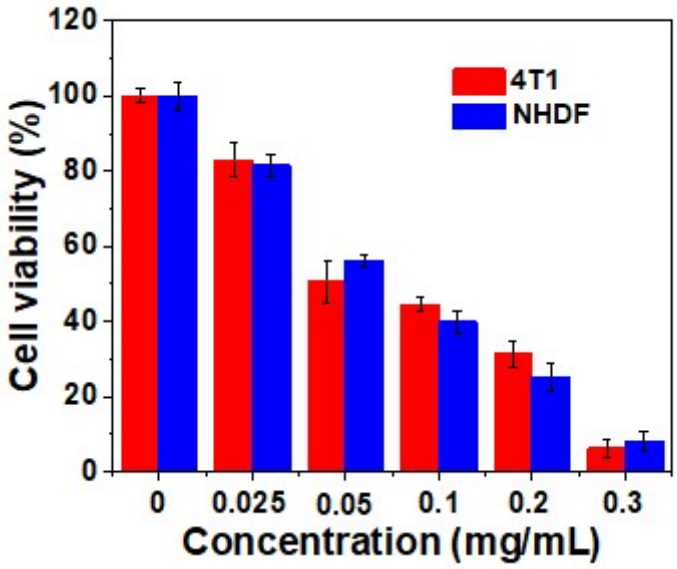

Fig. S11: The cytotoxicity of M-RP/BP@$ZnFe_2O_4$ NSs in 4T1 and NHDF cells under laser irradiation.

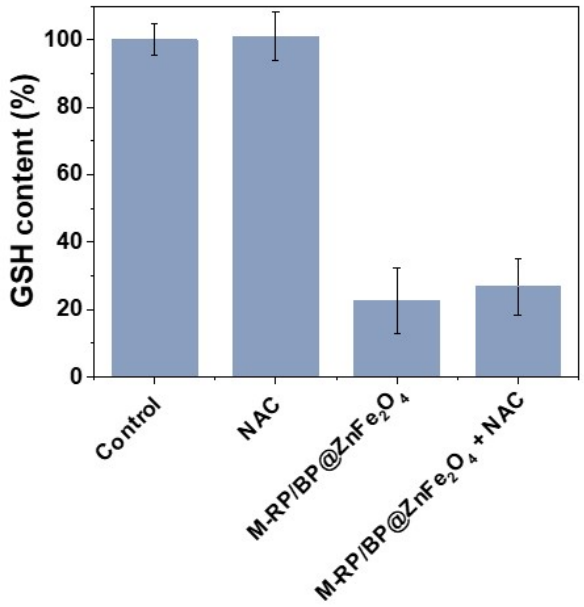

Fig. S12: GSH content of MCF-7 cells treated with PBS (control), NAC, M-RP/BP@$ZnFe_2O_4$ NSs and M-RP/BP@$ZnFe_2O_4$ NSs + NAC for 24 h.

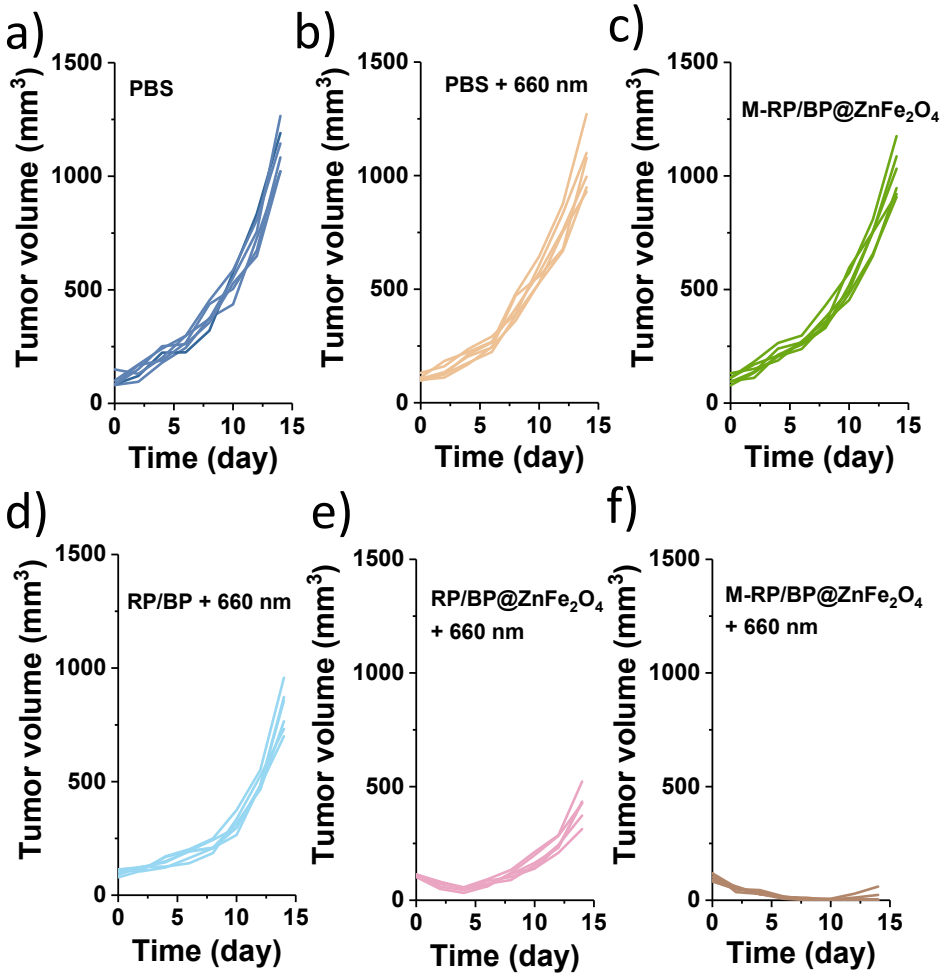

Fig. S13: a) Time-dependent tumor growth curves of MCF-7 tumor-bearing nude mice in control group. b) Time-dependent tumor growth curves of MCF-7 tumor-bearing nude mice in PBS + 660 nm laser group. c) Time-dependent tumor growth curves of MCF-7 tumor-bearing nude mice in M-RP/BP@$ZnFe_2O_4$ NSs group. d) Time-dependent tumor growth curves of MCF-7 tumor-bearing nude mice in RP/BP NSs + 660 nm laser group. e) Time-dependent tumor growth curves of MCF-7 tumor-bearing nude mice in RP/BP@$ZnFe_2O_4$ NSs + 660 nm laser group. f) Time-dependent tumor growth curves of MCF-7 tumor-bearing nude mice in M-RP/BP@$ZnFe_2O_4$ NSs + 660 nm laser group.

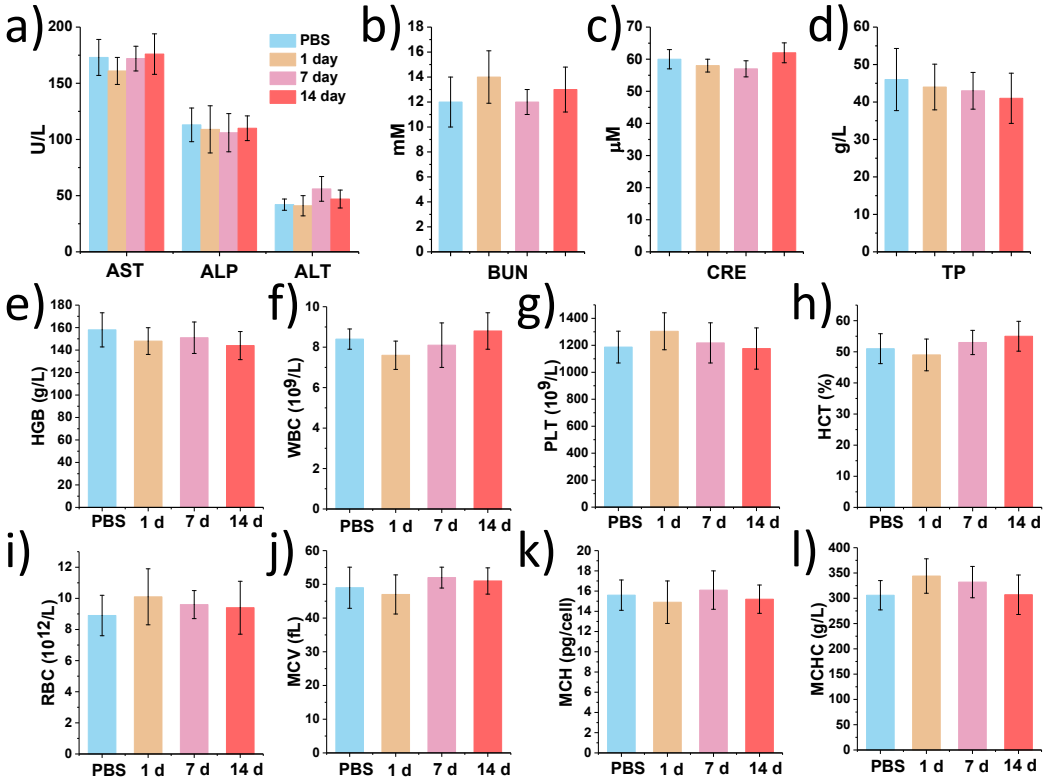

Fig. S14: Blood biochemical parameters of a) aspartate aminotransferase (AST), alkaline phosphatase (ALP) and aminotransferase (ALT), b) blood urea nitrogen(BUN), c) creatine (CRE) and d) total protein (TP) at 1, 7 and 14 days after intravenous injection of PBS and M-RP/BP@$ZnFe_2O_4$ NSs. The blood hematology data of e) hemoglobin (HGB), f) white blood cells (WBC), g) platelet (PLT), h) hematocrit (HCT), i) red blood cells (RBC), j) mean corpuscular volume (MCV), k) mean corpuscular hemoglobin (MCH) and l) corpuscular hemoglobin concentration (MCHC) at 1, 7 and 14 days after intravenous injection of PBS and M-RP/BP@$ZnFe_2O_4$ NSs.